

# Decoupling perturbations from background in $f(Q)$ gravity: the square-root correction and the alleviation of the $\sigma_8$ tension

**Chunyu Li,<sup>a,b</sup> Xin Ren,<sup>a,b</sup> Yuhang Yang,<sup>a,b</sup> Emmanuel N. Saridakis,<sup>c,b,d</sup> Yi-Fu Cai<sup>a,b</sup>**

<sup>a</sup>Department of Astronomy, School of Physical Sciences, University of Science and Technology of China, Hefei 230026, China

<sup>b</sup>CAS Key Laboratory for Research in Galaxies and Cosmology, School of Astronomy and Space Science, University of Science and Technology of China, Hefei 230026, China

<sup>c</sup>National Observatory of Athens, Lofos Nymfon 11852, Greece

<sup>d</sup>Departamento de Matemáticas, Universidad Católica del Norte, Avda. Angamos 0610, Casilla 1280, Antofagasta, Chile

E-mail: [springrain@mail.ustc.edu.cn](mailto:springrain@mail.ustc.edu.cn), [rx76@ustc.edu.cn](mailto:rx76@ustc.edu.cn),  
[yyh1024@mail.ustc.edu.cn](mailto:yyh1024@mail.ustc.edu.cn), [msaridak@noa.gr](mailto:msaridak@noa.gr), [yifucai@ustc.edu.cn](mailto:yifucai@ustc.edu.cn)

**Abstract.** We investigate a perturbation-level modification of symmetric teleparallel gravity of the form  $f(Q) = F(Q) + M\sqrt{Q}$  and assess its ability to ease the  $\sigma_8$  tension. The square-root term leaves the background expansion unchanged while modifying the effective gravitational coupling, providing a pure decoupling between background cosmology and structure-growth evolution. Using the latest redshift-space distortion data, including DESI DR2 Full-Shape measurements, we constrain  $M$  and  $\sigma_8$  across three representative backgrounds:  $\Lambda$ CDM, an  $H_0$ -tension-reducing model, and a DESI-motivated dynamical dark energy scenario. In all cases, the square-root correction suppresses growth and can reconcile  $\sigma_8$  with Planck at the  $1\sigma$  level, with the strongest improvement occurring in the  $H_0$ -tension-oriented background. A residual degeneracy between  $M$  and  $\sigma_8$  remains, indicating that future multi-probe analyses combining lensing and full-shape clustering will be required to determine whether the  $\sqrt{Q}$  term represents a genuine signal of modified gravity.

**Keywords:**  $f(Q)$  gravity,  $\sigma_8$  tension, Redshift-space distortions, DESI DR2

## 1 Introduction

The standard cosmological model, namely the  $\Lambda$ CDM paradigm, provides an excellent description of the Universe's evolution across a wide range of observations. Nevertheless, several persistent tensions have emerged as data precision has improved [1, 2]. The well-known  $H_0$  tension [3] highlights the discrepancy between the Hubble constant derived from early-universe Cosmic Microwave Background (CMB) measurements and late-universe supernova observations. Analogously, the  $S_8$  tension [4] manifests as a discrepancy in the parameter  $S_8 = \sigma_8 \sqrt{\Omega_m/0.3}$ , where  $\sigma_8$  denotes the amplitude of matter fluctuations at the scale of  $8h^{-1}$  Mpc and  $\Omega_m$  represents the matter density. Planck CMB measurements infer  $S_8 = 0.834 \pm 0.016$  [5], whereas large-scale structure (LSS) observations from galaxy clustering and weak lensing surveys consistently prefer lower values [6–11], resulting in a  $2\text{-}3\sigma$  tension. Ref. [4] demonstrated that this discrepancy is primarily driven by  $\sigma_8$  rather than  $\Omega_m$ . Consequently, in this work we focus on the  $\sigma_8$  (or, equivalently,  $S_8$ ) tension.

Modified gravity theories [12] provide a natural framework to address such cosmological tensions by altering both the background expansion history and the evolution of perturbations. Within this context, symmetric teleparallel gravity based on the non-metricity scalar  $Q$ , known as  $f(Q)$  gravity [13, 14], has emerged as a theoretically well-motivated candidate, with interesting cosmological phenomenology [15–51] (for a review see [52]). Symmetric teleparallel gravity includes General Relativity as a specific limit and has the advantage of second-order field equations. Previous studies have demonstrated that  $f(Q)$  models can effectively alleviate cosmological tensions [53–57]. However, late-time extensions that increase  $H_0$  typically reduce  $\sigma_8$  simultaneously, thereby exacerbating the growth tension, as discussed in [58]. This feature suggests that a viable framework should be able to modify  $\sigma_8$  and  $H_0$  in a controlled and, ideally, partially independent manner.

Working within the general framework of  $f(Q)$  gravity, we focus on the modification class

$$f(Q) = F(Q) + M\sqrt{Q},$$

as previously considered in [59–62], where the parameter  $M$  has units of  $[L^{-1}]$ . The inclusion of the  $\sqrt{Q}$  correction introduces a new degree of freedom with a distinctive and, for our purposes, crucial property: for homogeneous and isotropic backgrounds, this term cancels out of the modified Friedmann equations, leaving the background expansion history unchanged and thus preserving constraints from background observables. In contrast, the  $\sqrt{Q}$  term modifies the effective gravitational coupling  $G_{\text{eff}}$  and therefore directly affects the growth of linear perturbations. This decoupling between background and perturbation dynamics is highly non-generic in modified gravity theories and makes the model particularly suitable as a successful theoretical laboratory to investigate late-time clustering tensions in large-scale structure data.

Given that the  $M\sqrt{Q}$  correction specifically alters the evolution of perturbations without affecting the background dynamics, it is crucial to employ observational probes that are directly sensitive to structure formation. Redshift-space distortions (RSD) [63] are ideally suited for this purpose, as they constrain the growth rate of structure through the combination  $f\sigma_8(z)$ . Since RSD measurements provide a direct observational handle on density perturbations, they are expected to yield tight constraints on the  $\sqrt{Q}$  term and thus offer a robust test of the model's capability to alleviate the  $\sigma_8$  tension [55, 64–68]. In particular, the recent DESI

Full-Shape analysis [69] provides the most precise low-redshift measurements of  $f\sigma_8$  to date, significantly enhancing the constraining power on growth-modifying new physics.

Previous studies have explored related scenarios in  $f(Q)$  gravity. Ref. [59] constrained the parameters of the  $Q + M\sqrt{Q}$  model using RSD data, while Refs. [53, 60, 61] combined multiple cosmological probes to obtain broader constraints on  $f(Q)$  models. In the present work we advance these efforts in several directions. Firstly, we exploit the latest  $f\sigma_8$  measurements from DESI Full-Shape clustering [69] together with a robust compilation of RSD data to jointly constrain the  $M\sqrt{Q}$  term and  $\sigma_8$ , thereby directly testing the hypothesis that a perturbation-only modification can reconcile LSS data with Planck-inferred clustering amplitudes. Secondly, we investigate the interplay between the  $M\sqrt{Q}$  correction and different expansion histories by embedding the same  $\sqrt{Q}$  perturbation sector into three distinct  $f(Q)$  background models: (i) a model that reproduces the standard  $\Lambda$ CDM background, (ii) an exponential model that has been shown to alleviate the  $H_0$  tension, and (iii) a quadratic model realizing quintom dynamical dark energy, motivated by recent DESI results indicating that dark energy may evolve over time [70, 71]. This strategy allows us to assess to what extent a single perturbative degree of freedom can mitigate the  $\sigma_8$  tension across qualitatively different background cosmologies. At the quasi-static limit on small scales, i.e. the regime relevant to our analysis, the predictions of  $f(Q)$  and  $f(T)$  models coincide [13, 14], thus our results also have implications for torsional modified gravity.

The remainder of the paper is organized as follows. In Sec. 2, we review the theoretical framework of  $f(Q)$  gravity and outline the perturbation theory relevant for structure growth. In Sec. 3, we describe the observational datasets and the fitting methodology used in our analysis. Sec. 4 presents our parameter constraints and discusses the implications for the  $\sigma_8$  tension and the role of the  $M\sqrt{Q}$  term. Finally, Sec. 5 summarizes our conclusions and outlines possible directions for future tests.

## 2 $f(Q)$ gravity and cosmology

In this work we investigate modified gravity within the framework of  $f(Q)$  theories, where gravitational dynamics are governed by the non-metricity scalar  $Q$  rather than curvature or torsion [13, 14]. This section provides a concise overview of the geometrical foundations, background evolution, and perturbation dynamics relevant to our analysis, with particular emphasis on the distinctive role played by the square-root correction  $M\sqrt{Q}$ .

### 2.1 Geometry and field equations in $f(Q)$ gravity

The fundamental quantity of symmetric teleparallel gravity is the non-metricity tensor

$$Q_{\alpha\mu\nu} = \nabla_\alpha g_{\mu\nu} , \quad (2.1)$$

which implies that the vector lengths are not preserved under parallel transports. From this tensor one constructs the non-metricity scalar

$$Q = -Q_{\alpha\mu\nu} P^{\alpha\mu\nu} , \quad (2.2)$$

where the superpotential (or non-metricity conjugate)

$$P^\alpha{}_{\mu\nu} = -\frac{1}{2} L^\alpha{}_{\mu\nu} + \frac{1}{4} (Q^\alpha - \tilde{Q}^\alpha) g_{\mu\nu} - \frac{1}{4} \delta^\alpha_{(\mu} Q_{\nu)} , \quad (2.3)$$

is constructed from

$$L^\alpha_{\mu\nu} = \frac{1}{2} Q^\alpha_{\mu\nu} - Q_{(\mu\nu)}{}^\alpha, \quad (2.4)$$

with the two traces

$$Q_\alpha = g^{\mu\nu} Q_{\alpha\mu\nu}, \quad \tilde{Q}_\alpha = g^{\mu\nu} Q_{\mu\alpha\nu}. \quad (2.5)$$

Hence, the action of  $f(Q)$  gravity reads

$$\mathcal{S} = \int d^4x \sqrt{-g} \left[ -\frac{1}{16\pi G} f(Q) + \mathcal{L}_m \right], \quad (2.6)$$

where  $\mathcal{L}_m$  is the matter Lagrangian density.

## 2.2 Background dynamics

We adopt a spatially flat Friedmann-Lemaître-Robertson-Walker (FLRW) metric [13]

$$ds^2 = -dt^2 + a^2(t) \delta_{ij} dx^i dx^j, \quad (2.7)$$

for which the non-metricity scalar reduces to

$$Q = 6H^2, \quad H = \dot{a}/a. \quad (2.8)$$

Variation of the action (2.6) yields the modified Friedmann equations

$$6f_Q H^2 - \frac{f}{2} = 8\pi G \rho_m, \quad (2.9)$$

$$(12H^2 f_{QQ} + f_Q) \dot{H} = -4\pi G (\rho_m + p_m), \quad (2.10)$$

with  $\rho_m$  and  $p_m$  the energy density and pressure of the matter sector, assumed to correspond to an ideal fluid.

Let us now consider the form

$$f(Q) = F(Q) + M\sqrt{Q}. \quad (2.11)$$

As one can see by inserting (2.11) into the Friedmann equations, the square-root term cancels identically in both of them. Thus, the background evolution, namely the cosmological expansion history, depends solely on  $F(Q)$ , while  $M$  affects only perturbations. This feature is non-generic among modified gravity theories and is central to our study. Finally, we mention that imposing  $F(Q) = Q + 2\Lambda$  yields a  $\Lambda$ CDM background.

## 2.3 Linear perturbations and the effective gravitational coupling

Although the term  $M\sqrt{Q}$  leaves the background invariant, it modifies the evolution of scalar perturbations. In particular, in the Newtonian gauge

$$ds^2 = -(1 + 2\Psi)dt^2 + a^2(1 - 2\Phi)\delta_{ij} dx^i dx^j, \quad (2.12)$$

and in the subhorizon regime, where  $\Phi \simeq \Psi$  [72], the modified Poisson equation becomes

$$-k^2\Psi = 4\pi \frac{G_N}{f_Q} a^2 \rho_m \delta, \quad (2.13)$$

with  $\delta \equiv \delta\rho_m/\rho_m$  the matter overdensity.

The matter perturbation growth equation is

$$\ddot{\delta} + 2H\dot{\delta} - \frac{4\pi G_N}{f_Q} \rho_m \delta = 0, \quad (2.14)$$

implying an effective gravitational coupling of the form

$$G_{\text{eff}} = \frac{G_N}{f_Q}, \quad (2.15)$$

analogous to  $f(T)$  models [72, 73]. Since

$$f_Q = F_Q + \frac{M}{2\sqrt{Q}}, \quad (2.16)$$

a positive  $M$  increases  $f_Q$  and therefore reduces  $G_{\text{eff}}$ , producing a weaker effective gravity on growth scales, and thus suppressing structure formation, while a negative  $M$  enhances it. Hence, the parameter  $M$  serves as a pure perturbative handle for modifying the growth rate without changing  $H(z)$ .

## 2.4 Specific background realizations

In this subsection we summarize the three illustrative background choices used in our analysis. All models lie within the well-studied classes of symmetric teleparallel theories with no pathologies or instabilities. Each is compatible with the same perturbation-sector modification through  $M\sqrt{Q}$ .

### 2.4.1 Model A: $\Lambda$ CDM background

The simplest choice,

$$F_A(Q) = Q + 2\Lambda, \quad (2.17)$$

yields  $f(Q) = Q + M\sqrt{Q} + 2\Lambda$ . Additionally, note that equation (2.14) reduces to the general-relativity form when  $M = 0$ . We can re-write (2.14) using  $N = \ln a$  as the independent variable, namely

$$\delta'' + \delta' \left( 2 + \frac{H'}{H} \right) - \frac{3\sqrt{6}H}{2\sqrt{6}H + M} \Omega_m \delta = 0, \quad (2.18)$$

where primes denote derivatives with respect to  $N$  (hence  $\dot{\delta} = H\delta'$ ) and where we have introduced the matter density parameter  $\Omega_m = 8\pi G\rho_m/(3H^2)$ .

### 2.4.2 Model B: $H_0$ -tension alleviating background

A frequently studied form capable of enhancing late-time expansion [15, 55] is

$$F_B(Q) = Q e^{\beta Q_0/Q}, \quad (2.19)$$

with  $\beta$  and  $Q_0$  the model parameters. The normalized Hubble function  $E^2 = H^2/H_0^2$  (from now on the subscript “0” denotes the value of a quantity at present) satisfies

$$(E^2 - 2\beta)e^{\beta/E^2} = \Omega_{m0}a^{-3}, \quad (2.20)$$

with

$$\beta = \frac{1}{2} + W_0 \left( -\frac{\Omega_{m0}}{2\sqrt{e}} \right), \quad (2.21)$$

where  $W_0$  denotes the principal branch of the Lambert function. This background evolution approaches general relativity at high redshift (i.e. at  $Q \gg Q_0$ ), but it does not recover  $\Lambda$ CDM scenario at late times, hence it is a successful alternative to the latter, capable of alleviating the  $H_0$  tension [55, 56].

#### 2.4.3 Model C: Quintom dark energy background

Motivated by DESI indications of a quintom-like evolution of dark energy [74, 75], we consider the quadratic model

$$F_C(Q) = Q + \alpha_1 Q + \alpha_2 \frac{Q^2}{Q_0} - 2\alpha_3 Q_0, \quad (2.22)$$

shown to allow the effective equation-of-state parameter  $w(z)$  to cross  $-1$  [76–79]. This model provides a flexible dynamical dark energy sector, while remaining close to  $\Lambda$ CDM over the redshift range ( $z < 2$ ) relevant for our growth-rate analysis.

### 3 Observational data and methodology

Redshift-space distortions (RSD) constitute one of the most direct observational probes of the growth of cosmic structure. The peculiar velocities of galaxies introduce anisotropies in the observed clustering pattern, generating apparent distortions along the line of sight. Since these distortions are driven by the rate at which density perturbations grow under gravity, RSD measurements provide a robust test for probing deviations from general relativity and for constraining modified gravity scenarios such as the  $f(Q)$  models considered here.

#### 3.1 The observable $f\sigma_8$

As it is known, RSD measurements do not independently constrain the linear growth rate  $f$  or the clustering amplitude  $\sigma_8$ , but instead provide constraints on the combined observable

$$f\sigma_8(a) = \frac{d \ln \delta(a)}{d \ln a} \sigma_8(a) = \frac{\sigma_8(1)}{\delta(1)} a \frac{d \delta(a)}{da}, \quad (3.1)$$

where  $\sigma_8 \equiv \sigma_8(a = 1)$  is the present-day matter fluctuation amplitude at  $8h^{-1}\text{Mpc}$ . Expressed in terms of the number of e-folds  $N = \ln a$ , expression (3.1) becomes

$$f\sigma_8(N) = \frac{\delta'(N)}{\delta(N)} \sigma_8, \quad (3.2)$$

implying that any modification to the perturbation equation, such as that induced by the  $M\sqrt{Q}$  term in  $f(Q)$  gravity, directly affects the predicted  $f\sigma_8$  signal.

#### 3.2 RSD Dataset

The compilation of  $f\sigma_8(z)$  measurements used in this work is listed in Table 1. The first 22 data points correspond to the well-tested, internally robust dataset analyzed in [95], while the final six measurements are the recent DESI DR2 Full-Shape clustering results [69]. Together, they provide extensive redshift coverage and represent the most precise growth-rate measurements currently available, enabling stringent tests of the  $f(Q)$  models under consideration.

$z$	$f\sigma_8(z)$	$\sigma_{f\sigma_8}(z)$	$\Omega_{m,0}^{\text{ref}}$	Ref.
0.02	0.428	0.0465	0.3	[80]
0.02	0.398	0.065	0.3	[81], [82]
0.02	0.314	0.048	0.266	[83], [82]
0.10	0.370	0.130	0.3	[84]
0.15	0.490	0.145	0.31	[85]
0.17	0.510	0.060	0.3	[86]
0.18	0.360	0.090	0.27	[87]
0.38	0.440	0.060	0.27	[87]
0.25	0.3512	0.0583	0.25	[88]
0.37	0.4602	0.0378	0.25	[88]
0.32	0.384	0.095	0.274	[89]
0.59	0.488	0.060	0.307115	[90]
0.44	0.413	0.080	0.27	[91]
0.60	0.390	0.063	0.27	[91]
0.73	0.437	0.072	0.27	[91]
0.60	0.550	0.120	0.3	[92]
0.86	0.400	0.110	0.3	[92]
1.40	0.482	0.116	0.27	[93]
0.978	0.379	0.176	0.31	[94]
1.23	0.385	0.099	0.31	[94]
1.526	0.342	0.070	0.31	[94]
1.944	0.364	0.106	0.31	[94]
0.295	0.37784	0.09446	0.315	[69]
0.510	0.515879	0.061529	0.315	[69]
0.706	0.483315	0.055236	0.315	[69]
0.930	0.422208	0.046179	0.315	[69]
1.137	0.37468	0.037468	0.315	[69]
1.491	0.4350	0.045	0.315	[69]

**Table 1.** Compilation of the  $f\sigma_8(z)$  measurements used in this work.

### 3.3 Alcock-Paczyński Corrections

The Alcock-Paczyński effect arises when the conversion from observed redshifts to comoving distances assumes a fiducial cosmology different from the true one. Such geometric distortions induce anisotropies mimicking or modifying the RSD signal. If a measurement  $f\sigma'_8(z)$  is obtained under a fiducial Hubble parameter  $H'(z)$ , one must apply the correction [96, 97]

$$f\sigma_8(z) \simeq \frac{H(z)D_A(z)}{H'(z)D'_A(z)} f\sigma'_8(z) \equiv q(z, \Omega_{m0}, \Omega'_{m0}) f\sigma'_8(z), \quad (3.3)$$

where the angular diameter distance is

$$D_A(z) = \frac{1}{1+z} \int_0^z \frac{dz'}{H(z')}. \quad (3.4)$$

For realistic background cosmologies, the correction is mild, typically  $\sim 2\% - 3\%$  around  $z \sim 1$  [97]. Hence, to incorporate this correction consistently, we define the residual vector

$$V^i \equiv f\sigma_{8,i} - \frac{f\sigma_8(z_i, \Omega_{m0}, \sigma_8)}{q(z_i, \Omega_{m0}, \Omega_{m0}^{\text{fid}_i})}, \quad (3.5)$$

where  $f\sigma_{8,i}$  denotes the observed value and  $q$  is the Alcock-Paczyński factor.

### 3.4 Likelihood analysis

The total chi-squared used for parameter estimation is

$$\chi^2 = V^i C_{ij}^{-1} V^j, \quad (3.6)$$

where  $C_{ij}^{-1}$  is the inverse covariance matrix. All measurements are treated as uncorrelated except for the WiggleZ subsample, for which we use the published covariance matrix

$$C_{ij}^{\text{WiggleZ}} = 10^{-3} \begin{pmatrix} 6.400 & 2.570 & 0.000 \\ 2.570 & 3.969 & 2.540 \\ 0.000 & 2.540 & 5.184 \end{pmatrix}. \quad (3.7)$$

Now, in order to compare the performance of different models, we employ the Akaike (AIC) [98] and Bayesian (BIC) [99] information criteria, characterized by

$$\text{AIC} = -2 \ln L_{\max} + 2N_p, \quad (3.8)$$

$$\text{BIC} = -2 \ln L_{\max} + N_p \ln N_d, \quad (3.9)$$

where  $L_{\max}$  is the maximum likelihood,  $N_p$  is the number of model parameters, and  $N_d$  is the number of datapoints. Then, by calculating the differences  $\Delta\text{IC}$  relative to the model of reference, we have the following possibilities:  $\Delta\text{IC} < 2$  implies no preference and the two models are statistically equivalent;  $4 \lesssim \Delta\text{IC} \lesssim 7$  implies moderate support;  $\Delta\text{IC} > 10$  implies strong evidence.

### 3.5 Models and priors

As we mentioned above, we analyze three  $f(Q)$  models incorporating the same perturbation-sector correction  $M\sqrt{Q}$ , namely

$$\begin{aligned} \text{Model A : } & f(Q) = Q + 2\Lambda + M\sqrt{Q}, \\ \text{Model B : } & f(Q) = Q e^{\beta Q_0/Q} + M\sqrt{Q}, \\ \text{Model C : } & f(Q) = Q + \alpha_1 Q + \alpha_2 \frac{Q^2}{Q_0} - 2\alpha_3 Q_0 + M\sqrt{Q}. \end{aligned} \quad (3.10)$$

For each background, we consider the two cases, namely

1.  $M = 0$  (no perturbative modification),
2.  $M$  free and jointly constrained with  $\sigma_8$ .

Moreover, we adopt broad, flat priors:

$$\sigma_8 \in [0.6, 1.1], \quad M \in [-3H_0, 11H_0].$$

Note that since  $M$  has units of  $[L^{-1}]$ , i.e. of  $H$ , for convenience we measure it in  $(km \cdot s^{-1} \cdot Mpc^{-1})$ .

To ensure internal consistency, each background uses fiducial values  $(H_0, \Omega_{m0})$  corresponding to current best-fit constraints:

- i) Model A: (68.52, 0.2948) (DESI  $\Lambda$ CDM) [70],
- ii) Model B: (70.431, 0.3386), consistent with [55],
- iii) Model C: (68.03, 0.3085) (DESI  $w_0 w_a$ CDM).

Finally, note that for Model C we further use the background parameters  $\alpha_1 = -0.062, \alpha_2 = 0.003, \alpha_3 = -0.38$ , as obtained in [75].

Model	$\sigma_8$	$M(km \cdot s^{-1} \cdot Mpc^{-1})$	$\chi^2$	AIC	BIC	$\Delta$ AIC	$\Delta$ BIC
A	$0.784^{+0.022}_{-0.022}$	-	24.33	26.33	27.66	0	0
	$0.827^{+0.050}_{-0.045}$	$94.112^{+116.320}_{-87.442}$	22.99	26.99	29.65	0.66	1.99
B	$0.743^{+0.021}_{-0.021}$	-	31.50	33.50	34.83	7.17	7.17
	$0.847^{+0.035}_{-0.034}$	$280.601^{+130.838}_{-106.441}$	22.91	26.91	29.58	0.58	1.92
C	$0.788^{+0.022}_{-0.023}$	-	23.39	25.39	26.72	-0.94	-0.94
	$0.808^{+0.047}_{-0.042}$	$44.010^{+104.824}_{-80.039}$	23.06	27.06	29.73	0.73	2.07

**Table 2.** Best-fit values with 68% credible intervals for each model. Since  $M$  has units of  $[L^{-1}]$ , i.e. of  $H$ , for convenience we measure it in  $(km \cdot s^{-1} \cdot Mpc^{-1})$ . The first row of each model shows results for  $M = 0$ .

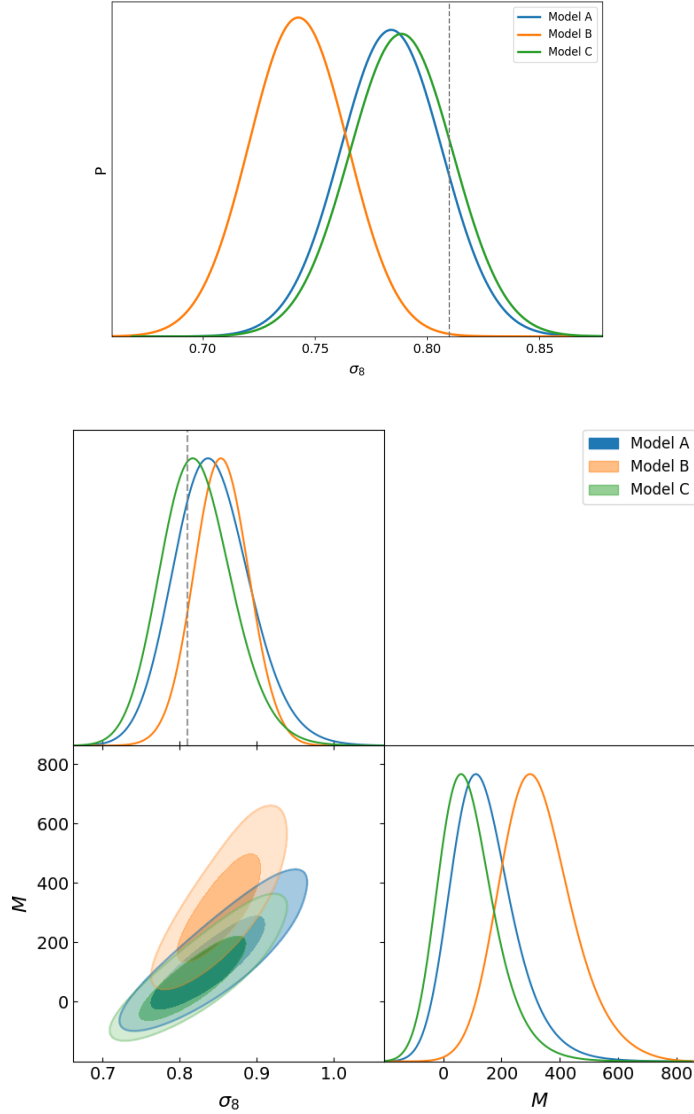


**Figure 1.** *Upper panel:* Constraints for  $\sigma_8$  values when  $M = 0$ ; *Lower panel:* Marginalised constraints for  $\sigma_8$  and  $M$  values at 68% and 95% C.L. The gray dashed line represents the value  $\sigma_8 = 0.81$ , which aligns with the Planck 2018 results.

## 4 Results and discussion

In this section we perform the observational confrontation as described above, and we discuss the obtained results. In Table 2 we summarize the best-fit values and information criteria for all scenarios considered. Furthermore, in Fig. 1 we present the posterior distributions of the free parameters. Let us now analyze the constraints on  $\sigma_8$  and  $M$  for each background model separately, and discuss their statistical interpretation and physical significance.

#### 4.1 Model A: $\Lambda$ CDM background

Model A reproduces the standard  $\Lambda$ CDM background expansion and therefore serves as a baseline reference. When  $M = 0$ , the RSD data prefer a slightly lower clustering amplitude than Planck, with  $\sigma_8$  falling  $1.18\sigma$  below the Planck 2018 value ( $\sigma_8 = 0.81$ ). This represents a statistically mild deviation, consistent with the well-documented tendency of low-redshift probes to favor weaker structure growth.

Allowing the square-root term to vary shifts the inferred  $\sigma_8$  upward, bringing it fully into agreement with Planck within  $1\sigma$ . However, the overall fit improvement is modest, and both AIC and BIC show only weak preference for the inclusion of  $M$ . Thus, for a  $\Lambda$ CDM background, the perturbation-only modification provided by  $M$  is not strictly required, although it can absorb the mild suppression of growth inferred from RSD data.

#### 4.2 Model B: Hubble-tension alleviating background

The behavior of Model B is qualitatively different. When constrained to  $M = 0$ , this model predicts a significantly lower  $\sigma_8$ , lying  $3.19\sigma$  below the Planck value. This reflects the fact that background modifications designed to increase  $H_0$ , as Model B does, typically reduce the growth rate, thereby intensifying the  $\sigma_8$  tension when considered alone.

However, introducing the square-root term changes this picture significantly. Once  $M$  is allowed to vary, the preferred value of  $\sigma_8$  rises and becomes entirely consistent with Planck at the  $1\sigma$  level. In parallel, the fit quality improves substantially. Both AIC and BIC decrease by more than seven units ( $\Delta\text{IC} > 7$ ), indicating strong statistical preference for including  $M$  as an additional parameter.

This result makes the key conceptual advantage of the  $\sqrt{Q}$  correction clear: it can restore compatibility with Planck-level clustering amplitudes in models whose background evolution would otherwise strongly suppress structure growth. In this sense, Model B with  $M \neq 0$  represents a highly successful example of using perturbative freedom to rescue an otherwise disfavored background scenario. This is one of the main results of the present work.

#### 4.3 Model C: Quintom dark energy background

Model C, based on a quadratic  $f(Q)$  form capable of generating a quintom-like equation of state, performs comparably to, or even slightly better than, the  $\Lambda$ CDM-based Model A. When  $M = 0$ , the preferred value of  $\sigma_8$  already lies close to the Planck result, with no significant tension.

Allowing  $M$  to vary does not alter this conclusion: the posterior distribution peaks near  $M = 0$ , indicating that the data do not favor an additional perturbative degree of freedom when quintom dark energy is already present in the background. This demonstrates that in Model C, the flexibility of the background evolution is sufficient to accommodate RSD measurements without requiring further modifications to  $G_{\text{eff}}$ .

Nonetheless, as shown in [70], this model does not resolve the Hubble tension once background observables are included. In particular, DESI BAO combined with Pantheon+ and CMB data yield  $H_0 = 68.03 \pm 0.72 \text{ km s}^{-1} \text{ Mpc}^{-1}$ , which remains in tension with local distance ladder measurements.

#### 4.4 Physical interpretation and parameter degeneracies

Let us now discuss the aforementioned results. As we can see, the square-root correction  $M\sqrt{Q}$  is theoretically notable because it modifies the growth of structure while leaving the background expansion unaltered. Our results show that a positive value of  $M$  suppresses the growth rate, equivalently reducing  $G_{\text{eff}}$ , and thereby compensates for the low-redshift preference for a suppressed  $f\sigma_8$ . This allows the intrinsic value of  $\sigma_8$  to remain closer to the Planck-inferred amplitude without compromising the agreement with RSD data.

As we observe from the posterior contours in Fig. 1, we obtain a degeneracy between  $M$  and  $\sigma_8$ . Increasing  $\sigma_8$  enhances the clustering amplitude, while increasing  $M$  suppresses the growth through a reduced effective gravitational strength. Their effects therefore counterbalance each other, producing elongated likelihood contours. This degeneracy explains why  $\sigma_8$  can shift towards higher values (appearing more consistent with Planck) when  $M$  is included: the perturbative modification absorbs the growth suppression required by low-redshift observations.

We should mention here that breaking this degeneracy will require incorporating complementary probes such as weak-lensing shear, CMB lensing, or full-shape galaxy spectra, all of which respond to  $G_{\text{eff}}$  and the growth history in different ways. Current RSD data, even with DESI DR2, are insufficient on their own to fully disentangle these effects.

In summary, our analysis confirms that the  $\sqrt{Q}$  correction provides a minimal and physically motivated perturbative mechanism capable of alleviating the  $\sigma_8$  tension across a wide range of background cosmologies, with especially strong impact in models that simultaneously aim to address the Hubble tension.

### 5 Conclusions

The persistent discrepancy between the clustering amplitude inferred from early-universe probes such as Planck and that measured by low-redshift large-scale structure surveys, continues to motivate the exploration of extensions to general relativity. Within this context, we investigated a class of symmetric teleparallel gravity models of the form  $f(Q) = F(Q) + M\sqrt{Q}$ , where the square-root correction introduces a new perturbative degree of freedom that modifies the effective gravitational coupling  $G_{\text{eff}}$  while leaving the background expansion history strictly unchanged. This feature makes the model a theoretically appealing and minimal candidate for addressing the  $S_8$  tension, as it isolates structure growth modifications from the background cosmology.

Using the latest set of redshift-space distortion measurements, including DESI DR2 Full-Shape constraints, we carried out a systematic parameter estimation analysis across three representative background scenarios: (i) a  $\Lambda$ CDM background (Model A), (ii) a modified expansion designed to alleviate the Hubble tension (Model B), and (iii) a quintom dark-energy background motivated by recent DESI reconstructions (Model C). Our findings can be summarized as follows.

For Model A ( $\Lambda$ CDM background), we were expecting that taking  $M = 0$  we recover completely the standard cosmological paradigm, which already shows only a mild ( $1.18\sigma$ ) deviation from the Planck value of  $\sigma_8$ , consistent with known low-redshift trends. Introducing

the  $M\sqrt{Q}$  correction further improves this agreement, bringing  $\sigma_8$  within  $1\sigma$  of Planck. Although the statistical preference for  $M \neq 0$  is modest, this scenario demonstrates that the perturbative correction can fine-tune growth dynamics without altering the background.

In the case of Model B (Hubble-tension-oriented background), we found that the square-root correction displays its most significant impact in this scenario. When  $M = 0$ , the model predicts a value of  $\sigma_8$  that deviates from Planck by  $3.19\sigma$ , placing it in strong tension with growth-rate data. However, once the square-root term is activated, the discrepancy is fully removed, and  $\sigma_8$  becomes consistent with Planck at the  $1\sigma$  level. Both AIC and BIC strongly favor the inclusion of  $M$ , indicating that perturbative modifications are essential to recover compatibility with data in this background. This result highlights the capacity of  $M\sqrt{Q}$  to rescue background cosmologies that would otherwise be disfavored by structure formation measurements, and is the main result of this work.

In the case of Model C (quintom dark energy), we showed that the model achieves the best overall statistical performance, with the lowest AIC and BIC values. However, the posterior peaks near  $M = 0$ , showing that the baseline dynamical background already matches the RSD data without requiring additional perturbative freedom. Nonetheless, this scenario does not resolve the Hubble tension, consistent with recent Gaussian-process reconstructions based on DESI DR2, Pantheon+, and compressed CMB data.

Our theoretical analysis confirms that a positive value of  $M$  suppresses the linear growth of structure by reducing the effective gravitational strength. This mechanism naturally reconciles the lower clustering amplitude preferred by low-redshift data with the higher amplitude favored by early-time physics. Crucially, this indicates that the square-root correction is not just a phenomenological patch but a physically interpretable modification capable of jointly addressing the  $H_0$  and  $S_8$  tensions within a unified  $f(Q)$  framework.

At the same time, the results reveal an extended degeneracy between  $M$  and  $\sigma_8$ , as is clearly visible in the posterior contours. This degeneracy reflects the competing effects between enhanced intrinsic clustering and suppressed growth through  $G_{\text{eff}}$ . Its presence reveals the possible limitations of current RSD datasets, which still suffer from relatively large uncertainties, partial inconsistencies among surveys, and a notable sensitivity to the choice of fiducial cosmology (especially  $\Omega_m$ ). These issues currently hinder a precise determination of  $M$  using RSD alone.

Recent developments strengthen this perspective. Studies based on the cosmic shear three-point correlation function [100] and EFTofLSS analyses [101] suggest that improved non-linear modeling within  $\Lambda$ CDM may also reduce the tension. This indicates that the origin of the  $S_8$  anomaly may arise from a combination of late-time gravitational physics, non-linear structure formation, and observational systematics. Distinguishing between these possibilities is a central open challenge.

We close this work by mentioning that to break the degeneracy between  $M$  and  $\sigma_8$  and decisively test the physical relevance of the square-root correction, upcoming work must incorporate complementary probes. In particular, weak-lensing measurements, full-shape galaxy clustering, higher-order statistics, redshift-space multipoles, and CMB lensing, respond differently to modifications of  $G_{\text{eff}}$  and to the evolution of matter perturbations. Future multi-probe analyses, especially those combining Euclid, DESI Year 2+, Rubin LSST, and CMB-S4 data, will dramatically enhance sensitivity to perturbative gravitational effects. On the the-

oretical side, assessing the stability, screening behavior, and cosmological consistency of the square-root sector, will further clarify whether this modification represents a viable extension of symmetric teleparallel gravity. In conclusion, considered together, these observational and theoretical efforts will be crucial for determining whether the  $M\sqrt{Q}$  correction constitutes a genuine physical signature or an artifact resulting from the current stage of cosmological modeling.

## Acknowledgments

We are grateful to Qingqing Wang, Yating Peng for insightful comments. This work was supported in part by the National Key R&D Program of China (2021YFC2203100, 2024YFC2207500), by the National Natural Science Foundation of China (12433002, 12261131497, 92476203), by CAS young interdisciplinary innovation team (JCTD-2022-20), by 111 Project (B23042), by Anhui Postdoctoral Scientific Research Program Foundation (No. 2025C1184), by CSC Innovation Talent Funds, by USTC Fellowship for International Cooperation, and by USTC Research Funds of the Double First-Class Initiative. ENS acknowledges the contribution of the LISA CosWG and the COST Actions and of COST Actions CA21136 “Addressing observational tensions in cosmology with systematics and fundamental physics (CosmoVerse)”, CA21106 “COSMIC WISPerS in the Dark Universe: Theory, astrophysics and experiments (CosmicWISPerS)”, and CA23130 “Bridging high and low energies in search of quantum gravity (BridgeQG)”.

## References

- [1] COSMOVERSE NETWORK collaboration, *The CosmoVerse White Paper: Addressing observational tensions in cosmology with systematics and fundamental physics*, *Phys. Dark Univ.* **49** (2025) 101965 [[2504.01669](#)].
- [2] L. Perivolaropoulos and F. Skara, *Challenges for  $\Lambda$ CDM: An update*, *New Astron. Rev.* **95** (2022) 101659 [[2105.05208](#)].
- [3] E. Di Valentino et al., *Snowmass2021 - Letter of interest cosmology intertwined II: The hubble constant tension*, *Astropart. Phys.* **131** (2021) 102605 [[2008.11284](#)].
- [4] E. Di Valentino et al., *Cosmology Intertwined III:  $f\sigma_8$  and  $S_8$* , *Astropart. Phys.* **131** (2021) 102604 [[2008.11285](#)].
- [5] PLANCK collaboration, *Planck 2018 results. VI. Cosmological parameters*, *Astron. Astrophys.* **641** (2020) A6 [[1807.06209](#)].
- [6] S. Joudaki et al., *KiDS-450: Testing extensions to the standard cosmological model*, *Mon. Not. Roy. Astron. Soc.* **471** (2017) 1259 [[1610.04606](#)].
- [7] H. Hildebrandt et al., *KiDS-450: Cosmological parameter constraints from tomographic weak gravitational lensing*, *Mon. Not. Roy. Astron. Soc.* **465** (2017) 1454 [[1606.05338](#)].
- [8] DES collaboration, *Dark Energy Survey Year 1 results: Cosmological constraints from cosmic shear*, *Phys. Rev. D* **98** (2018) 043528 [[1708.01538](#)].
- [9] C. Heymans et al., *KiDS-1000 Cosmology: Multi-probe weak gravitational lensing and spectroscopic galaxy clustering constraints*, *Astron. Astrophys.* **646** (2021) A140 [[2007.15632](#)].
- [10] KiDS collaboration, *KiDS-1000 Cosmology: Cosmic shear constraints and comparison between two point statistics*, *Astron. Astrophys.* **645** (2021) A104 [[2007.15633](#)].
- [11] T. Tröster et al., *Cosmology from large-scale structure: Constraining  $\Lambda$ CDM with BOSS*, *Astron. Astrophys.* **633** (2020) L10 [[1909.11006](#)].

[12] CANTATA collaboration, E.N. Saridakis et al., *Modified Gravity and Cosmology. An Update by the CANTATA Network*, Springer (2021), [10.1007/978-3-030-83715-0](https://doi.org/10.1007/978-3-030-83715-0), [[2105.12582](#)].

[13] J. Beltrán Jiménez, L. Heisenberg and T. Koivisto, *Coincident General Relativity*, *Phys. Rev. D* **98** (2018) 044048 [[1710.03116](#)].

[14] J. Beltrán Jiménez, L. Heisenberg, T.S. Koivisto and S. Pekar, *Cosmology in  $f(Q)$  geometry*, *Phys. Rev. D* **101** (2020) 103507 [[1906.10027](#)].

[15] F.K. Anagnostopoulos, S. Basilakos and E.N. Saridakis, *First evidence that non-metricity  $f(Q)$  gravity could challenge  $\Lambda$ CDM*, *Phys. Lett. B* **822** (2021) 136634 [[2104.15123](#)].

[16] R. Lazkoz, F.S.N. Lobo, M. Ortiz-Baños and V. Salzano, *Observational constraints of  $f(Q)$  gravity*, *Phys. Rev. D* **100** (2019) 104027 [[1907.13219](#)].

[17] J. Lu, X. Zhao and G. Chee, *Cosmology in symmetric teleparallel gravity and its dynamical system*, *Eur. Phys. J. C* **79** (2019) 530 [[1906.08920](#)].

[18] S. Mandal, D. Wang and P.K. Sahoo, *Cosmography in  $f(Q)$  gravity*, *Phys. Rev. D* **102** (2020) 124029 [[2011.00420](#)].

[19] G.N. Gadbail, S. Mandal and P.K. Sahoo, *Reconstruction of  $\Lambda$ CDM universe in  $f(Q)$  gravity*, *Phys. Lett. B* **835** (2022) 137509 [[2210.09237](#)].

[20] W. Khyllep, A. Paliathanasis and J. Dutta, *Cosmological solutions and growth index of matter perturbations in  $f(Q)$  gravity*, *Phys. Rev. D* **103** (2021) 103521 [[2103.08372](#)].

[21] M. Hohmann, *General covariant symmetric teleparallel cosmology*, *Phys. Rev. D* **104** (2021) 124077 [[2109.01525](#)].

[22] S. Mandal and P.K. Sahoo, *Constraint on the equation of state parameter ( $\omega$ ) in non-minimally coupled  $f(Q)$  gravity*, *Phys. Lett. B* **823** (2021) 136786 [[2111.10511](#)].

[23] S. Capozziello and R. D'Agostino, *Model-independent reconstruction of  $f(Q)$  non-metric gravity*, *Phys. Lett. B* **832** (2022) 137229 [[2204.01015](#)].

[24] R. Solanki, A. De and P.K. Sahoo, *Complete dark energy scenario in  $f(Q)$  gravity*, *Phys. Dark Univ.* **36** (2022) 100996 [[2203.03370](#)].

[25] S.A. Narawade, L. Pati, B. Mishra and S.K. Tripathy, *Dynamical system analysis for accelerating models in non-metricity  $f(Q)$  gravity*, *Phys. Dark Univ.* **36** (2022) 101020 [[2203.14121](#)].

[26] S. Capozziello and M. Shokri, *Slow-roll inflation in  $f(Q)$  non-metric gravity*, *Phys. Dark Univ.* **37** (2022) 101113 [[2209.06670](#)].

[27] H. Shabani, A. De, T.-H. Loo and E.N. Saridakis, *Cosmology of  $f(Q)$  gravity in non-flat Universe*, *Eur. Phys. J. C* **84** (2024) 285 [[2306.13324](#)].

[28] J. Ferreira, T. Barreiro, J. Mimoso and N.J. Nunes, *Forecasting  $F(Q)$  cosmology with  $\Lambda$ CDM background using standard sirens*, *Phys. Rev. D* **105** (2022) 123531 [[2203.13788](#)].

[29] S. Arora and P.K. Sahoo, *Crossing Phantom Divide in  $f(Q)f(Q)$  Gravity*, *Annalen Phys.* **534** (2022) 2200233 [[2206.05110](#)].

[30] A. Paliathanasis, *Dynamical analysis of  $fQ$ -cosmology*, *Phys. Dark Univ.* **41** (2023) 101255 [[2304.04219](#)].

[31] R. D'Agostino and R.C. Nunes, *Forecasting constraints on deviations from general relativity in  $f(Q)$  gravity with standard sirens*, *Phys. Rev. D* **106** (2022) 124053 [[2210.11935](#)].

[32] A. De and T.-H. Loo, *On the viability of  $f(Q)$  gravity models*, *Class. Quant. Grav.* **40** (2023) 115007 [[2212.08304](#)].

[33] J. Beltrán Jiménez and T.S. Koivisto, *Lost in translation: The Abelian affine connection (in the coincident gauge)*, *Int. J. Geom. Meth. Mod. Phys.* **19** (2022) 2250108 [[2202.01701](#)].

[34] A. De, T.-H. Loo and E.N. Saridakis, *Non-metricity with boundary terms:  $f(Q, C)$  gravity and cosmology*, *JCAP* **03** (2024) 050 [[2308.00652](#)].

[35] M. Koussour and A. De, *Observational constraints on two cosmological models of  $f(Q)$  theory*, *Eur. Phys. J. C* **83** (2023) 400 [[2304.11765](#)].

[36] C.G. Boehmer, E. Jensko and R. Lazkoz, *Dynamical Systems Analysis of  $f(Q)$  Gravity*, *Universe* **9** (2023) 166 [[2303.04463](#)].

[37] R. Bhagat, S.A. Narawade and B. Mishra, *Weyl type  $f(Q, T)$  gravity observational constrained cosmological models*, *Phys. Dark Univ.* **41** (2023) 101250 [[2305.01659](#)].

[38] G.N. Gadbail, A. De and P.K. Sahoo, *Cosmological reconstruction and  $\Lambda$ CDM universe in  $f(Q, C)$  gravity*, *Eur. Phys. J. C* **83** (2023) 1099 [[2312.02492](#)].

[39] H. Shabani, A. De and T.-H. Loo, *Phase-space analysis of a novel cosmological model in  $f(Q)$  theory*, *Eur. Phys. J. C* **83** (2023) 535 [[2304.02949](#)].

[40] S.V. Lohakare, S.K. Maurya, K.N. Singh, B. Mishra and A. Errehymy, *Influence of three parameters on maximum mass and stability of strange star under linear  $f(Q)$  – action*, *Mon. Not. Roy. Astron. Soc.* **526** (2023) 3796 [[2309.10830](#)].

[41] A. Paliathanasis, N. Dimakis and T. Christodoulakis, *Minisuperspace description of  $f(Q)$ -cosmology*, *Phys. Dark Univ.* **43** (2024) 101410 [[2308.15207](#)].

[42] J. Shi, *Cosmological constraints in covariant  $f(Q)$  gravity with different connections*, *Eur. Phys. J. C* **83** (2023) 951 [[2307.08103](#)].

[43] K. Hu, T. Paul and T. Qiu, *Tensor perturbations from bounce inflation scenario in  $f(Q)$  gravity*, *Sci. China Phys. Mech. Astron.* **67** (2024) 220413 [[2308.00647](#)].

[44] N. Dimakis, A. Paliathanasis and T. Christodoulakis, *Quantum cosmology in  $f(Q)$  theory*, *Class. Quant. Grav.* **38** (2021) 225003 [[2108.01970](#)].

[45] F.K. Anagnostopoulos, V. Gakis, E.N. Saridakis and S. Basilakos, *New models and big bang nucleosynthesis constraints in  $f(Q)$  gravity*, *Eur. Phys. J. C* **83** (2023) 58 [[2205.11445](#)].

[46] A. Lymeris, *Late-time cosmology with phantom dark-energy in  $f(Q)$  gravity*, *JCAP* **11** (2022) 018 [[2207.10997](#)].

[47] Y. Yang, X. Ren, B. Wang, Y.-F. Cai and E.N. Saridakis, *Data reconstruction of the dynamical connection function in  $f(Q)$  cosmology*, *Mon. Not. Roy. Astron. Soc.* **533** (2024) 2232 [[2404.12140](#)].

[48] F. D'Ambrosio, L. Heisenberg and S. Zentarra, *Hamiltonian Analysis of  $f(Q)f(Q)$  Gravity and the Failure of the Dirac–Bergmann Algorithm for Teleparallel Theories of Gravity*, *Fortsch. Phys.* **71** (2023) 2300185 [[2308.02250](#)].

[49] M.-J. Guzmán, L. Järv and L. Pati, *Exploring the stability of  $f(Q)$  cosmology near general relativity limit with different connections*, *Phys. Rev. D* **110** (2024) 124013 [[2406.11621](#)].

[50] S. Capozziello and M. Capriolo, *Gravitational waves in  $f(Q)$  non-metric gravity without gauge fixing*, *Phys. Dark Univ.* **45** (2024) 101548 [[2405.16163](#)].

[51] S. Basilakos, A. Paliathanasis and E.N. Saridakis, *Equivalence of  $f(Q)$  cosmology with quintom-like scenario: The phantom field as effective realization of the non-trivial connection*, *Phys. Lett. B* **868** (2025) 139658 [[2503.19864](#)].

[52] L. Heisenberg, *Review on  $f(Q)$  gravity*, *Phys. Rept.* **1066** (2024) 1 [[2309.15958](#)].

[53] Z. Sakr and L. Schey, *Investigating the Hubble tension and  $\sigma_8$  discrepancy in  $f(Q)$  cosmology*, *JCAP* **10** (2024) 052 [[2405.03627](#)].

[54] Q. Wang, X. Ren, Y.-F. Cai, W. Luo and E.N. Saridakis, *Observational Test of  $f(Q)$  Gravity with Weak Gravitational Lensing*, *Astrophys. J.* **974** (2024) 7 [[2406.00242](#)].

[55] C.G. Boiza, M. Petronikolou, M. Bouhmadi-López and E.N. Saridakis, *Addressing  $H_0$  and  $S_8$  tensions within  $f(Q)$  cosmology*, [2505.18264](#).

[56] J.A. Nájera, I. Banik, H. Desmond and V. Kalaitzidis, *Background solutions to the Hubble tension in  $f(Q)$  gravity and consistency with BAO measurements*, [2510.20964](#).

[57] N.S. Kavya, S.S. Mishra and P.K. Sahoo,  *$f(q)$  gravity as a possible resolution of the  $h_0$  and  $s_8$  tensions with desi dr2*, *Scientific Reports* **15** (2025) .

[58] L. Heisenberg, H. Villarrubia-Rojo and J. Zosso, *Can late-time extensions solve the  $H_0$  and  $\sigma_8$  tensions?*, *Phys. Rev. D* **106** (2022) 043503 [[2202.01202](#)].

[59] B.J. Barros, T. Barreiro, T. Koivisto and N.J. Nunes, *Testing  $F(Q)$  gravity with redshift space distortions*, *Phys. Dark Univ.* **30** (2020) 100616 [[2004.07867](#)].

[60] N. Frusciante, *Signatures of  $f(Q)$ -gravity in cosmology*, *Phys. Rev. D* **103** (2021) 044021 [[2101.09242](#)].

[61] L. Atayde and N. Frusciante, *Can  $f(Q)$  gravity challenge  $\Lambda$ CDM?*, *Phys. Rev. D* **104** (2021) 064052 [[2108.10832](#)].

[62] A. Kolhatkar, S.S. Mishra and P.K. Sahoo, *Implications of cosmological perturbations of  $\sqrt{Q}$  in STEGR*, *Eur. Phys. J. C* **85** (2025) 656.

[63] N. Kaiser, *Clustering in real space and in redshift space*, *Mon. Not. Roy. Astron. Soc.* **227** (1987) 1.

[64] B.J. Barros, L. Amendola, T. Barreiro and N.J. Nunes, *Coupled quintessence with a  $\Lambda$ CDM background: removing the  $\sigma_8$  tension*, *JCAP* **01** (2019) 007 [[1802.09216](#)].

[65] G. Lambiase, S. Mohanty, A. Narang and P. Parashari, *Testing dark energy models in the light of  $\sigma_8$  tension*, *Eur. Phys. J. C* **79** (2019) 141 [[1804.07154](#)].

[66] A. Gómez-Valent and J. Solà Peracaula, *Density perturbations for running vacuum: a successful approach to structure formation and to the  $\sigma_8$ -tension*, *Mon. Not. Roy. Astron. Soc.* **478** (2018) 126 [[1801.08501](#)].

[67] S.-F. Yan, P. Zhang, J.-W. Chen, X.-Z. Zhang, Y.-F. Cai and E.N. Saridakis, *Interpreting cosmological tensions from the effective field theory of torsional gravity*, *Phys. Rev. D* **101** (2020) 121301 [[1909.06388](#)].

[68] J. Solà Peracaula, A. Gómez-Valent, J. de Cruz Pérez and C. Moreno-Pulido, *Brans-Dicke cosmology with a  $\Lambda$ -term: a possible solution to  $\Lambda$ CDM tensions*, *Class. Quant. Grav.* **37** (2020) 245003 [[2006.04273](#)].

[69] DESI collaboration, *DESI 2024 V: Full-Shape galaxy clustering from galaxies and quasars*, *JCAP* **09** (2025) 008 [[2411.12021](#)].

[70] DESI collaboration, *DESI 2024 VI: cosmological constraints from the measurements of baryon acoustic oscillations*, *JCAP* **02** (2025) 021 [[2404.03002](#)].

[71] DESI collaboration, *DESI DR2 Results II: Measurements of Baryon Acoustic Oscillations and Cosmological Constraints*, [2503.14738](#).

[72] R. Zheng and Q.-G. Huang, *Growth factor in  $f(T)$  gravity*, *JCAP* **03** (2011) 002 [[1010.3512](#)].

[73] S. Bahamonde, V. Gakis, S. Kiorpelidi, T. Koivisto, J. Levi Said and E.N. Saridakis, *Cosmological perturbations in modified teleparallel gravity models: Boundary term extension*, *Eur. Phys. J. C* **81** (2021) 53 [[2009.02168](#)].

[74] Y. Yang, X. Ren, Q. Wang, Z. Lu, D. Zhang, Y.-F. Cai et al., *Quintom cosmology and modified gravity after DESI 2024*, *Sci. Bull.* **69** (2024) 2698 [[2404.19437](#)].

[75] Y. Yang, Q. Wang, X. Ren, E.N. Saridakis and Y.-F. Cai, *Modified Gravity Realizations of Quintom Dark Energy after DESI DR2*, *Astrophys. J.* **988** (2025) 123 [[2504.06784](#)].

[76] B. Feng, X.-L. Wang and X.-M. Zhang, *Dark energy constraints from the cosmic age and supernova*, *Phys. Lett. B* **607** (2005) 35 [[astro-ph/0404224](#)].

[77] D. Huterer and A. Cooray, *Uncorrelated estimates of dark energy evolution*, *Phys. Rev. D* **71** (2005) 023506 [[astro-ph/0404062](#)].

[78] Y.-F. Cai, E.N. Saridakis, M.R. Setare and J.-Q. Xia, *Quintom Cosmology: Theoretical implications and observations*, *Phys. Rept.* **493** (2010) 1 [[0909.2776](#)].

[79] Y. Cai, X. Ren, T. Qiu, M. Li and X. Zhang, *The Quintom theory of dark energy after DESI DR2*, [2505.24732](#).

[80] D. Huterer, D. Shafer, D. Scolnic and F. Schmidt, *Testing  $\Lambda$ CDM at the lowest redshifts with SN Ia and galaxy velocities*, *JCAP* **05** (2017) 015 [[1611.09862](#)].

[81] S.J. Turnbull, M.J. Hudson, H.A. Feldman, M. Hicken, R.P. Kirshner and R. Watkins, *Cosmic flows in the nearby universe from Type Ia Supernovae*, *Mon. Not. Roy. Astron. Soc.* **420** (2012) 447 [[1111.0631](#)].

[82] M.J. Hudson and S.J. Turnbull, *The growth rate of cosmic structure from peculiar velocities at low and high redshifts*, *Astrophys. J. Lett.* **751** (2013) L30 [[1203.4814](#)].

[83] M. Davis, A. Nusser, K. Masters, C. Springob, J.P. Huchra and G. Lemson, *Local Gravity versus Local Velocity: Solutions for  $\beta$  and nonlinear bias*, *Mon. Not. Roy. Astron. Soc.* **413** (2011) 2906 [[1011.3114](#)].

[84] M. Feix, A. Nusser and E. Branchini, *Growth Rate of Cosmological Perturbations at  $z \sim 0.1$  from a New Observational Test*, *Phys. Rev. Lett.* **115** (2015) 011301 [[1503.05945](#)].

[85] C. Howlett, A. Ross, L. Samushia, W. Percival and M. Manera, *The clustering of the SDSS main galaxy sample – II. Mock galaxy catalogues and a measurement of the growth of structure from redshift space distortions at  $z = 0.15$* , *Mon. Not. Roy. Astron. Soc.* **449** (2015) 848 [[1409.3238](#)].

[86] Y.-S. Song and W.J. Percival, *Reconstructing the history of structure formation using Redshift Distortions*, *JCAP* **10** (2009) 004 [[0807.0810](#)].

[87] C. Blake et al., *Galaxy And Mass Assembly (GAMA): improved cosmic growth measurements using multiple tracers of large-scale structure*, *Mon. Not. Roy. Astron. Soc.* **436** (2013) 3089 [[1309.5556](#)].

[88] L. Samushia, W.J. Percival and A. Raccanelli, *Interpreting large-scale redshift-space distortion measurements*, *Monthly Notices of the Royal Astronomical Society* **420** (2012) 2102.

[89] BOSS collaboration, *The clustering of galaxies in the SDSS-III Baryon Oscillation Spectroscopic Survey: cosmological implications of the full shape of the clustering wedges in the data release 10 and 11 galaxy samples*, *Mon. Not. Roy. Astron. Soc.* **440** (2014) 2692 [[1312.4854](#)].

[90] BOSS collaboration, *The clustering of galaxies in the SDSS-III Baryon Oscillation Spectroscopic Survey: single-probe measurements from CMASS anisotropic galaxy clustering*, *Mon. Not. Roy. Astron. Soc.* **461** (2016) 3781 [[1312.4889](#)].

[91] C. Blake, S. Brough, M. Colless, C. Contreras, W. Couch, S. Croom et al., *The wigglez dark energy survey: Joint measurements of the expansion and growth history at  $z \geq 1$* , *Monthly Notices of the Royal Astronomical Society* **425** (2012) 405.

[92] A. Pezzotta et al., *The VIMOS Public Extragalactic Redshift Survey (VIPERS): The growth of structure at  $0.5 < z < 1.2$  from redshift-space distortions in the clustering of the PDR-2 final sample*, *Astron. Astrophys.* **604** (2017) A33 [[1612.05645](#)].

[93] T. Okumura et al., *The Subaru FMOS galaxy redshift survey (FastSound). IV. New constraint*

*on gravity theory from redshift space distortions at  $z \sim 1.4$ , *Publ. Astron. Soc. Jap.* **68** (2016) 38* [[1511.08083](#)].

[94] EBOSS collaboration, *The clustering of the SDSS-IV extended Baryon Oscillation Spectroscopic Survey DR14 quasar sample: a tomographic measurement of cosmic structure growth and expansion rate based on optimal redshift weights*, *Mon. Not. Roy. Astron. Soc.* **482** (2019) 3497 [[1801.03043](#)].

[95] B. Sagredo, S. Nesseris and D. Sapone, *Internal Robustness of Growth Rate data*, *Phys. Rev. D* **98** (2018) 083543 [[1806.10822](#)].

[96] E. Macaulay, I.K. Wehus and H.K. Eriksen, *Lower Growth Rate from Recent Redshift Space Distortion Measurements than Expected from Planck*, *Phys. Rev. Lett.* **111** (2013) 161301 [[1303.6583](#)].

[97] L. Kazantzidis and L. Perivolaropoulos, *Evolution of the  $f\sigma_8$  tension with the Planck15/ΛCDM determination and implications for modified gravity theories*, *Phys. Rev. D* **97** (2018) 103503 [[1803.01337](#)].

[98] H. Akaike, *A new look at the statistical model identification*, *IEEE transactions on automatic control* **19** (2003) 716.

[99] G. Schwarz, *Estimating the dimension of a model*, *The annals of statistics* (1978) 461.

[100] DES collaboration, *Dark Energy Survey Year 3 Results: Cosmological constraints from second and third-order shear statistics*, [2508.14018](#).

[101] G. D'Amico, A. Refregier, L. Senatore and P. Zhang, *The cosmological analysis of DES 3×2pt data from the Effective Field Theory of Large-Scale Structure*, [2510.24878](#).